

Relaxation Spectrum of Polymer Networks Formed from Butyl Acrylate and Methyl Methacrylate Monomeric Units

A. Espadero Berzosa,[†] J. L. Gómez Ribelles,^{*,†} S. Kripotou,[‡] and P. Pissis[‡]

Center for Biomaterials, Universidad Politécnica de Valencia, Camino de Vera s/n, E-46071 Valencia, Spain, and Department of Physics, National Technical University of Athens, Zografou Campus, 15780 Athens, Greece

Received March 23, 2004; Revised Manuscript Received June 4, 2004

ABSTRACT: The aim of this work is to study the merging of the main α and the secondary β relaxations in poly(butyl acrylate)-*i*-poly(methyl methacrylate) sequential interpenetrating networks in comparison to *net*-poly(butyl acrylate)-*co*-poly(methyl methacrylate) random copolymer networks. In both cases 10% of ethylene glycol dimethacrylate was used as cross-linking agent. The cross-linking density of these networks is high enough to force a certain degree of compatibility of the IPNs, as shown by dynamic-mechanical analysis and thermally stimulated depolarization currents, TSDC. Dielectric relaxation spectroscopy was used to characterize the relaxation behavior in the frequency domain. The strength of the α dielectric relaxation in poly(methyl methacrylate) network is small and the merging with the β relaxation is not apparent in the experimental frequency range. On the contrary, in poly(butyl acrylate) networks it is the strength of the secondary relaxation which is small compared to that of the α relaxation and the relaxation spectrum has the characteristics of the latter in the whole experimental temperature interval. In the copolymer networks, the introduction of butyl acrylate segments in the polymer chains shifts the α process toward lower temperatures with respect to poly(methyl methacrylate) and increases the relaxation strength of the α relaxation. The crossover region is shown in copolymers with methyl methacrylate content ranging between 20 and 60 wt %. Nevertheless, in the IPNs with similar compositions the relaxation spectrum shows the characteristics of a secondary relaxation. This behavior is ascribed to the fact that the glass transition of the IPN is dispersed in an extremely broad temperature range, so its relaxation strength at each temperature is quite small, being not significant in comparison to that of the β relaxation.

Introduction

The molecular mobility of poly(alkyl methacrylate)s has been extensively studied using dielectric relaxation spectroscopy. Already in 1966 G. Williams¹ stated that the main α relaxation and the secondary β relaxation merge, at temperatures above the glass transition temperature T_g , in a new $\alpha\beta$ relaxation process which has characteristics different from both α and β relaxation; i.e., it is not a mere superposition of both processes. The crossover region is the frequency–temperature region in which the relaxation times of the α and β processes approach each other. An extensive analysis of the knowledge and different points of view on the way of evaluating the contribution of each component to the overall relaxation process can be found in refs 2 to 8. The merging of the main and the secondary dielectric relaxations could be a general phenomenon in amorphous polymers as has been proved using broadband dielectric spectroscopy.^{9,10}

The permanent dipolar moment that resides in poly(alkyl methacrylate)s and poly(alkyl acrylate)s in the carboxyl group of the side chain can be reoriented under the presence of an electric field by the cooperative conformational rearrangements of the segments of the polymer chains, but even when these motions are not possible, some reorientation can be also achieved by rotation of the side chain with respect to its bond with the main chain. This fact produces that the main α relaxation and the β relaxation in these polymers are

not independent from each other. It has been shown that as the length of the side chain increases the strength of the main relaxation, $\Delta\epsilon_\alpha$, increases while that of the secondary relaxation, $\Delta\epsilon_\beta$, decreases.^{1–4,10–15} In the crossover region, when the temperature decreases the first motions that are frozen are the cooperative conformational rearrangements responsible for the α relaxation. The dielectric activity at temperatures below the glass transition depends on the ability to reorient the side chains in the glassy state, the β relaxation has to do with the loss of this residual mobility on further decreasing temperature. Thus, the strength of the β relaxation in atactic polymers with bulky side groups is small because nearly all the ability to reorient the permanent dipole is lost in the α relaxation, when going through the glass transition. The relationship between $\Delta\epsilon_\alpha$ and $\Delta\epsilon_\beta$ is further proved by its dependence on the pressure applied to the sample above T_g .^{1,2} When increasing pressure $\Delta\epsilon_\beta$ decreases while $\Delta\epsilon_\alpha$ increases keeping $\Delta\epsilon = \Delta\epsilon_\alpha + \Delta\epsilon_\beta$ constant. Depending on the existence of other permanent dipolar moments in the side chains, some polymers of these series can present low-temperature secondary relaxations called γ , δ , etc. in decreasing order of temperature.

At temperatures below the calorimetric glass transition the α relaxation would appear at extremely low frequencies and consequently the behavior of the β relaxation can be characterized with no influence of the cooperative conformational rearrangements of the main chains. In this temperature range, that we will call hereafter the c regime,⁴ the β relaxation appears nearly at the same temperature and with the same apparent activation energy in the series of poly(alkyl methacryl-

* To which correspondence should be addressed.

[†] Universidad Politécnica de Valencia.

[‡] National Technical University of Athens.

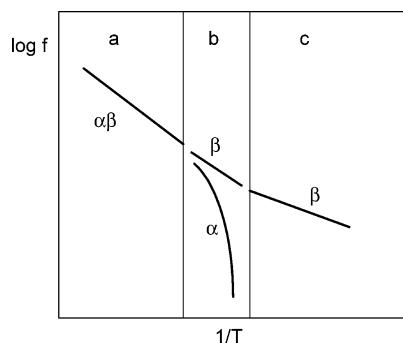


Figure 1. Scheme of an Arrhenius diagram showing the merging of the α and β relaxations of a poly(alkyl methacrylate).

ate)s.^{1–4,10–15} There is a temperature interval in which the α and β relaxations overlap, the b regime. The characteristics of each relaxation process in this zone are difficult to know with enough accuracy, since the separation of the contributions of the α and β components is still controversial.^{2,4–8,16,17} Anyway, it seems to be accepted that the α relaxation presents the characteristics of a cooperative motion: the curvature of the Arrhenius diagram follows the Vogel–Fulcher–Tammann–Hesse, VFTH, equation,^{18–20} while the β relaxation still shows a temperature independent apparent activation energy although higher than in the c regime. At higher temperatures the α and β relaxations merge in the $\alpha\beta$ process with an Arrhenius behavior, with higher apparent activation energy than the β relaxation in regime b but with a relaxation strength that decreases with increasing temperature.^{1–7,21} Figure 1 shows a scheme of the Arrhenius diagram of a poly(alkyl methacrylate).

The cooperative character of α , β , and $\alpha\beta$ relaxations in the different temperature regions can be analyzed studying the influence of the presence of a second component (in the form of a copolymer, a polymer blend or an interpenetrated polymer network) on the mobility of the polymer chain segments. Random copolymers of different alkyl methacrylates showed the same features as the poly(alkyl methacrylate) series with properties corresponding to a number of methyl units in the side chain intermediate between that of the components according to the copolymer composition.³ Kahle et al.⁶ studied the dielectric relaxation spectrum of poly(*n*-butyl methacrylate-*stat*-styrene) copolymers and found a continuous shift of the onset temperature and frequency of the α relaxation varying the styrene content of the copolymer. Zhang et al.²² reported a clear shift of the α relaxation of PEMA toward high temperatures when blending with poly(4-vinylphenol) with little change in the β relaxation but a significant increase of the apparent activation energy of the $\alpha\beta$ relaxation as the content of PEMA in the blend decreased.

The merging region in poly(butyl acrylate)-*i*-poly(butyl methacrylate), PBA-*i*-PBMA, or poly(ethyl acrylate)-*i*-poly(ethyl methacrylate), PEA-*i*-PEMA sequential interpenetrated polymer networks was studied in refs 16, 17, and 21. Polyacrylate–polymethacrylate pairs are immiscible except for very low molecular weight polymers,²³ but single phase interpenetrated polymer networks with the same components in the network form can be obtained if the cross-linking density is high enough.^{16,17,21,24,25} The compatibilized IPNs present an extremely broad glass transition. Thus, a poly(methyl acrylate)-*i*-poly(methyl methacrylate) IPN cross-linked

with 10% EGDMA shows a single glass transition in DSC covering a temperature interval of around 100 deg.²⁵

The aim of this work is to compare the merging of the α and β relaxations in poly(butyl acrylate)-*i*-poly(methyl methacrylate) highly cross-linked interpenetrated polymer networks with that of poly(butyl acrylate)-*stat*-poly(methyl methacrylate) random copolymer networks with the same cross-linking density.

Experimental Section

Sequential interpenetrated polymeric networks (IPN) were prepared by bulk copolymerization using benzoin as photoinitiator (0.2%) and ethylene glycol dimethacrylate, EDGMA, as cross-linker (10%) for both networks. The poly(butyl acrylate) network was polymerized first to form a 0.4 mm thick sheet. Afterward, this network was immersed and swollen in a solution of methyl methacrylate, MMA, in ethanol containing benzoin (0.2 wt % with respect to MMA) and EGDMA (10% with respect to MMA) and allowed to swell to equilibrium (24 h). By variation of the weight ratio MMA/ethanol, IPNs of different composition were obtained. The polymerization of the second (net-PMMA) network took place then under UV light. The sheets thus obtained were boiled in ethanol to extract residual monomer and other low-molecular weight substances, and dried in vacuo, at a temperature above the expected T_g of the sample, to constant weight.

The series of IPNs obtained covered only a limited composition interval. The net-PBA content in the IPN ranged from 40 to 60 wt %. The limit compositions were obtained when the MMA/ethanol ratios in the solution employed to form the second network were 0.9 and 0.5, respectively. Lower concentrations of ethanol in the solution caused internal tensions in the swollen sample, causing its break. Concentrations of ethanol higher than 50% in the swelling solution lead to a nonhomogeneous sample.

Copolymer networks were prepared also by bulk copolymerization, using 0.2% of benzoin as initiator and 10% of EGDMA as cross-linking agent. The weight ratios butyl acrylate/methyl methacrylate were 0.2, 0.4, 0.6, and 0.8. Polymerization took place under UV light for 24 h, and then the samples were boiled in ethanol and dried in vacuo to constant weight.

Also networks of the pure components were synthesized, with the same content of photoinitiator and cross-linker.

Sequential IPNs will be designated as IPNXX, XX being the weight percentage of *net*-PBA in the IPN. Copolymer networks will be designated as COPZZ, ZZ being the weight percent of butyl acrylate units in the copolymer.

Dielectric relaxation spectroscopy (DRS) was performed in a Schlumberger frequency response analyzer FRA SI1 260 with a range of 10^{-2} – 10^6 Hz. The sample was clamped between two gold electrodes in a dielectric cell, which was introduced inside a cryostatic Novocontrol system. The experimental temperature interval covered from -60 to $+200$ °C. The samples were measured between 0.1 and 10^6 Hz typically every 10 deg in the appropriate temperature range for each sample.

Dynamic-mechanical analysis, DMA, was carried out in a Seiko DMS210 instrument at 1 Hz.

For thermally stimulated depolarization currents (TSDC), a dielectric technique in the temperature domain,²⁶ the Novocontrol TSDC cell and the cryostatic system were used. The sample was clamped between two golden electrodes. The depolarization current was measured by means of a Keithley 617 electrometer as a function of temperature in the range from about -100 to about $+150$ °C.

Results

As a representative plot of the dynamic-mechanical results, Figure 2a shows the temperature dependence of the loss tangent of the homopolymer and copolymer networks. The *net*-PMMA clearly shows the β and α

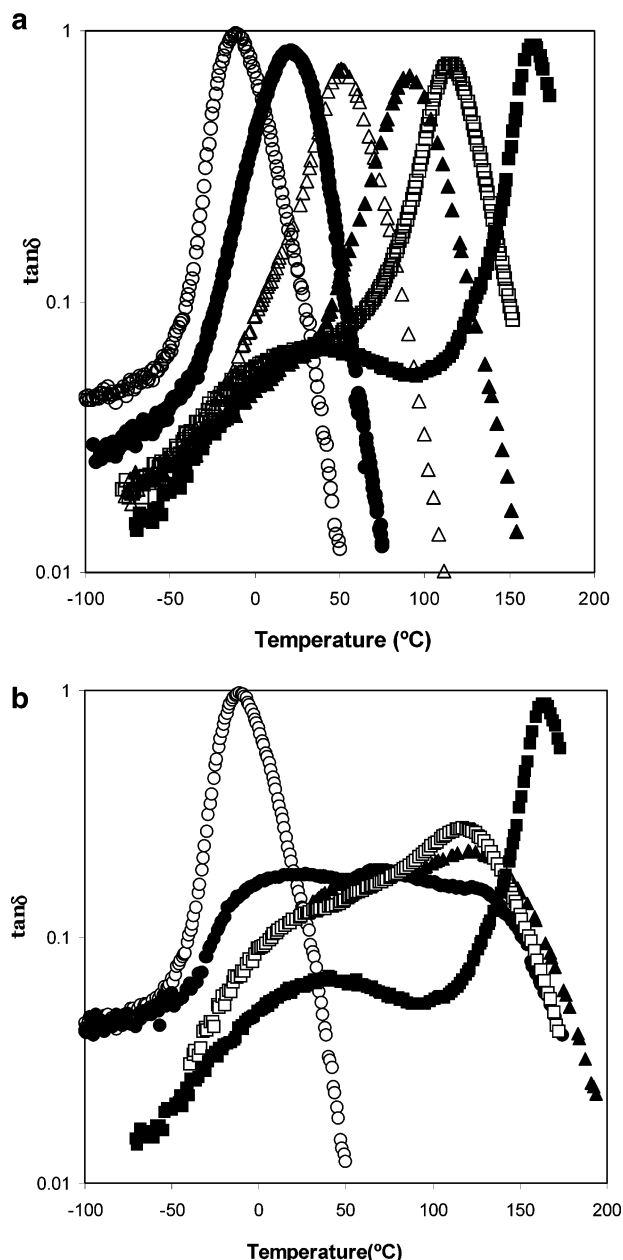


Figure 2. (a) Temperature dependence of the mechanical loss tangent of the homopolymer and copolymer networks: (■) *net*-PMMA, (□) COP20, (▲) COP40, (△) COP 60, (●) COP80, and (○) *net*-PBA. (b) Loss tangent of the sequential IPNs: (■) *net*-PMMA, (□) IPN42, (▲) IPN50, (●) IPN59, and (○) *net*-PBA.

relaxations. The secondary relaxation appears as a broad peak with a maximum at 40 °C. The maximum of $\tan \delta$ corresponding to the α relaxation (we will call $T_{\alpha\text{DMA}}$ the temperature of the maximum of the loss tangent measured at 1 Hz) appears at 163 °C. The *net*-PBA presents only the α relaxation in the temperature interval of our experiments, with a maximum of the loss tangent at $T_{\alpha\text{DMA,PBA}} = -11$ °C.

The copolymer networks show the α relaxation at a temperature $T_{\alpha\text{DMA}}$ that monotonically increases as the MMA contents of the copolymer increases, in a manner similar to the expected dependence of the glass transition temperature on composition for a random copolymer.

The β relaxation, due to the motion of the side chains, only appears as a shoulder in those copolymers with a high content of MMA units (COP 20 and COP40).

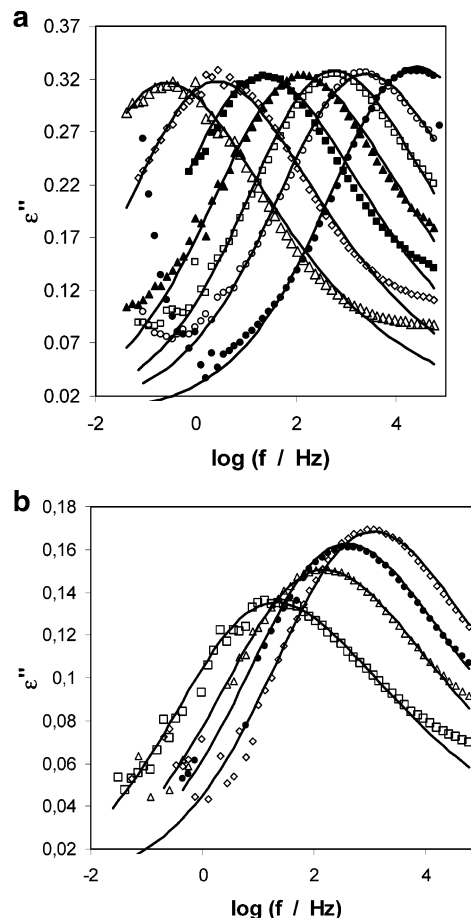


Figure 3. Representative isotherms of the imaginary part of the complex dielectric permittivity: (a) measured in *net*-PBA at (△) −35, (◇) −30, (■) −25, (▲) −20, (□) −15, (○) −10, and (●) 0 °C; (b) measured in IPN42 at (□) 20, (△) 40, (●) 50, and (◇) 60 °C. The solid lines correspond to the Havriliak–Negami equation.

The IPNs present an extremely broad relaxation peak that is probably the consequence of the overlapping of several relaxation processes (Figure 2b). A shoulder in the low-temperature side of the relaxation peak seems to correspond to the secondary relaxation but the shape of the high-temperature side also shows the superposition of more than one relaxation process. Nevertheless, there is no sign of relaxation in the temperature intervals in which the α relaxation of the pure component networks takes place.

The imaginary component of the dielectric permittivity measured at constant temperature in the frequency domain showed a single peak for all the networks and in the whole temperature interval (Figure 3 shows two representative examples corresponding to the PBA network and the IPN containing 42% of BA units). The Havriliak–Negami²⁷ function was used to fit the experimental results,

$$\epsilon^*(\omega) - \epsilon_\infty = \frac{\Delta\epsilon}{(1 + (i\omega\tau_0)^{1-a})^b} \quad (2)$$

where $\Delta\epsilon$ is the relaxation strength, ϵ_∞ is the limit to high frequencies of the real component of the complex permittivity, ϵ^* , ω is the angular frequency, τ_0 plays the role of a time constant, and a and b are shape parameters.

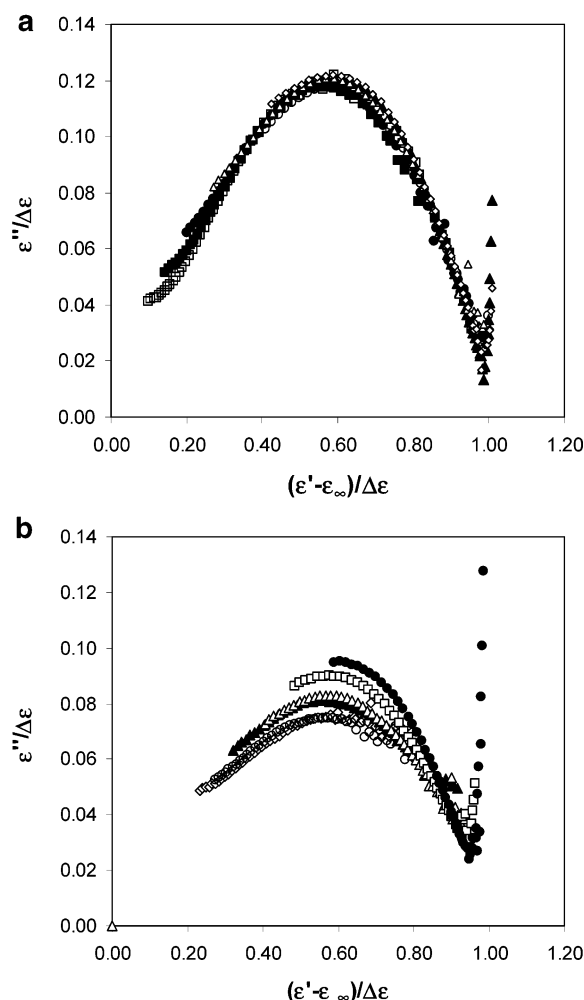


Figure 4. Reduced Cole–Cole diagrams for the polymer and copolymer networks. (a) *net*-PBA: (□) -30 , (■) -25 , (●) -20 , (Δ) -15 , (○) -10 , (◇) -5 , and (▲) 0 °C. (b) COP60: (◇) 10 , (○) 20 , (▲) 30 , (Δ) 40 , (□) 50 , and (●) 60 °C.

In the case of PBA network, the secondary relaxation is far enough from the main relaxation. Figure 3a shows that the shape of the ϵ'' isotherms does not change with temperature, what is indicative of a thermorheologically simple behavior of the pure α relaxation in this polymer. To further clarify this point a reduced master Cole–Cole arc was built, as shown in Figure 4a, in which $\epsilon''/\Delta\epsilon$ is represented against $(\epsilon' - \epsilon_\infty)/\Delta\epsilon$. For each temperature it was possible to find a value of the relaxation strength that makes the corresponding Cole–Cole arc to superpose on the master curve. Clearly the shape of the relaxation and consequently the values of the parameters $a = 0.63$ and $b = 0.54$ of the HN equation are temperature independent. Interestingly enough, the relaxation strength was temperature independent as well, with a value of $\Delta\epsilon = 2.7$.

The same procedure was followed with copolymer containing 80% of PBA, COP80. The normalized Cole–Cole arc (results not shown) is a master curve and the values of the parameters $a = 0.7$ and $b = 0.55$ are temperature independent. Now the relaxation strength increases with temperature (Figure 5).

The same procedure conducted on the results of the rest of networks did not yield a master curve (as an example Figure 4c shows the reduced Cole–Cole arcs for COP60). The values of the a parameter decreased

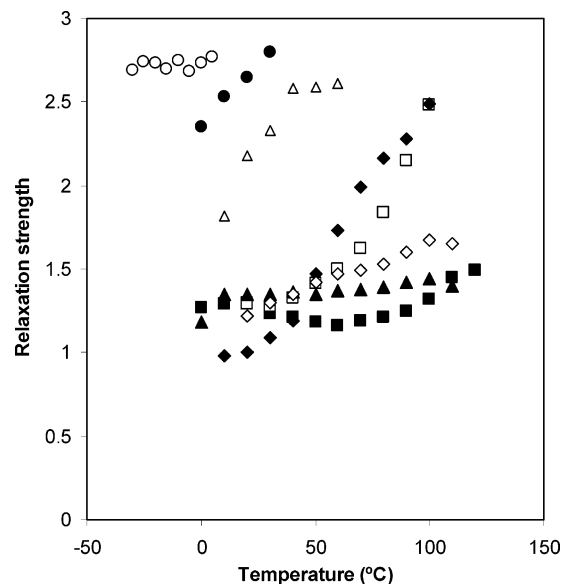


Figure 5. Dependence of the relaxation strength on temperature of the different networks and IPNs: (■) *net*-PMMA, (□) COP20, (◆) COP40, (Δ) COP 60, (●) COP80, (○) *net*-PBA, (◇) IPN42, and (▲) IPN50.

with temperature (the parameter a changed from 0.6 to 0.45 between 10 and 120 °C in *net*-PMMA, from 0.62 to 0.57 between 20 and 90 °C in COP20, from 0.71 to 0.66 between 10 and 100 °C in COP40 and from 0.75 to 0.69 between 10 and 60 °C in COP60), while b is nearly constant in all the networks. The result in the case of PMMA is not surprising, since the shape of the secondary relaxation must not be temperature independent, and the same may happen in the copolymers containing 40% or more PMMA. In these cases the relaxation strength was determined from the HN fit to each individual isotherm. The fact that the HN curve does not fit exactly the experimental isotherm in the high-frequency tail of the relaxation means that the value $\Delta\epsilon$ obtained in the fitting procedure could be slightly underestimated, nevertheless any other method of extrapolation in the Cole–Cole diagram based only on the shape of the curve at high frequencies would need new assumptions which would be difficult to justify.

To complete the description of the set of DRS results the temperature dependence of the frequency of the characteristic maximum in ϵ'' is represented in the Arrhenius plot of Figure 6.

Dielectric relaxation was investigated by an additional dielectric technique, namely TSDC. This technique consists of measuring the stored dielectric polarization and it corresponds to measuring dielectric losses against temperature at constant equivalent frequencies in the range 10^{-2} – 10^{-4} Hz. The technique is characterized by high sensitivity and high resolving power²⁶ and it has already been used to investigate the relaxational behavior of methacrylates²⁸ and miscibility in polymer blends.²⁹

Figure 7 shows TSDC thermograms for the homopolymer and the copolymer networks in the temperature region of interest. Similar to DMA, two relaxations are observed in *net*-PMMA, the α relaxation at about 140 °C and the broad β relaxation at about -40 °C, whereas only one relaxation, the α relaxation, is observed at about -40 °C in the *net*-PBA. The copolymers show also two relaxations: a broad α relaxation systematically shifting to higher temperatures with de-

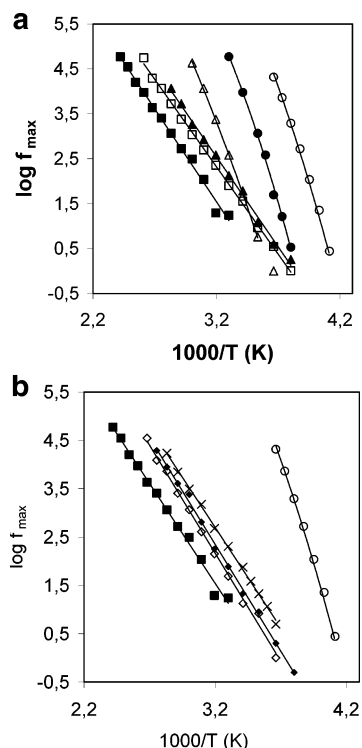


Figure 6. Arrhenius diagram showing the position of the relaxation peaks in the frequency axis at different temperatures: (a) (■) *net*-PMMA, (□) COP20, (◆) COP40, (△) COP 60, (●) COP80, and (○) *net*-PBA; (b) (■) *net*-PMMA, (◇) IPN42, (▲) IPN50, (×) IPN59, and (○) *net*-PBA. The lines in this plots correspond to the Arrhenius behavior in the case of secondary relaxations and to the VFTH equation in the case of pure α relaxations.

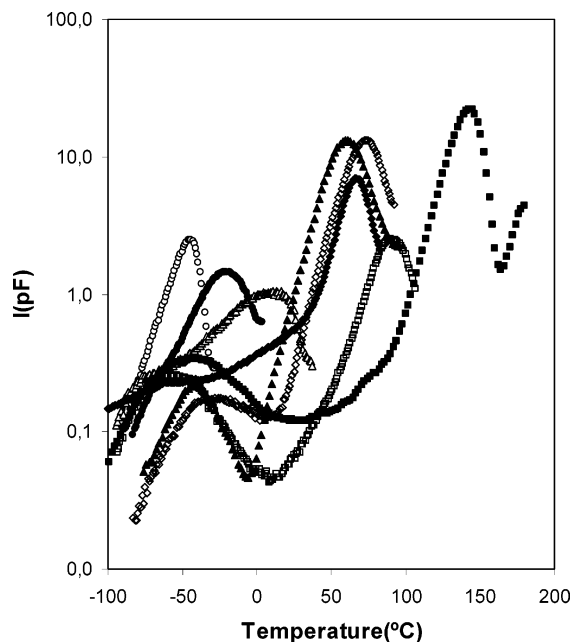


Figure 7. TSDC thermograms obtained with the homopolymer and copolymer networks and two IPNs indicated on the plot: (■) *net*-PMMA, (□) COP20, (◆) COP40, (△) COP 60, (●) COP80, (○) *net*-PBA, (◇) IPN42, and (▲) IPN59. Only one datum point per degree has been represented for clarity.

creasing PBA content and a weaker relaxation in the temperature region of the β relaxation of *net*-PMMA, which for COP80 and COP60 becomes a shoulder on the low-temperature side of the α relaxation. The magnitude of α peak is a measure of the strength of the corre-

sponding relaxation. However, conductivity may contribute to the α peak, depending on the polarization conditions, and affect both temperature position and magnitude of the peak. Special TSDC techniques can then be employed to isolate dipolar from conductivity contributions,³⁰ this point being not further followed here.

The TSDC thermograms for two IPNs, IPN42 and IPN59, are also shown in Figure 7. Similar to the copolymers, two peaks are observed in the IPN thermograms. The one at higher temperatures is shifted toward the PMMA α peak, with respect to the corresponding copolymer peak, whereas that at lower temperatures looks more similar to the PBA α peak than the PMMA β peak, both effects being more clear for IPN59 than for IPN42.

Discussion

The main difference between the α relaxation process observed in the highly cross-linked *net*-PBA and that of chain polymers is the independence of the relaxation strength from temperature, at least in the temperature interval in which confident data of $\Delta\epsilon$ can be obtained (between -30 and 0 °C). Probably at higher temperatures $\Delta\epsilon$ starts decreasing, since the low-frequency limit of ϵ' is in this network a slightly decreasing function of temperature above 0 °C as happens in chain polymers. Nevertheless, it is not possible to obtain reliable extrapolations of ϵ_∞ at so high temperatures, even using the criterium of superposing the isotherm on the master reduced Cole–Cole arc of Figure 4. In a series of poly(methyl acrylate) networks³¹ with varying cross-linking densities, a similar feature was found. The relaxation strength of the main dielectric relaxation decreased with increasing temperature in loosely cross-linked networks but the networks prepared with high amounts of cross-linking agent showed much smaller changes of $\Delta\epsilon(T)$ which present a clear maximum. This behavior was attributed to the increase of the influence of the secondary relaxation with respect to α relaxation as cross-linking density increases. The case of the PBA networks of this work is different, since there is no sign of the secondary relaxation of this network in the temperature window of the experiments. It was shown¹⁵ that the strength of the β relaxation of the polymers of the series of poly(*n*-alkyl acrylate)s decreases with increasing the length of the side chain and in PBA it is difficult to detect.

Other characteristics of the main dielectric relaxation in this network are those of the cooperative conformational motions of the polymer chain segments. The position of the maxima of ϵ'' in the frequency axis shows the VFTH behavior (Figure 6). The α relaxation is asymmetric, the shape of the distribution of relaxation times being independent of temperature as shown by the constancy of the parameters a and b of the HN equation and the master Cole–Cole arc shown in Figure 4a.

On the contrary, the relaxation observed in *net*-PMMA presents the characteristics of the secondary β relaxation. The apparent activation energy calculated from the plot of Figure 5 is 72 kJ/mol. The relaxation strength slightly increases with increasing temperature. The strength of the α relaxation is small, compared to that of β relaxation, and it has not been possible to identify clearly the temperature interval in which the merging of the α and β relaxation takes place and to

Table 1. Apparent Activation Energies of the Secondary Relaxation and Parameters of the VFTH Equation for the α Relaxation^a

	E_A (kJ/mol)	A	B (K)	T_0 (K)	T_α (°C)	a	b
net-PBA		17.55	1685	145	-10	0.63	0.54
COP80		14.87	1374	168	20	0.7	0.55
COP60		16.39	2341	133	50	0.74	0.54
COP40	77				90	0.69	0.55
COP20	75				117	0.57	0.47
net-PMMA	79				165	0.45 ^b	0.45
IPN42	86				125	0.57	0.46
IPN50	85				125	0.57	0.49
IPN60	79						

^a The shape parameters of the HN equation at a temperature 20 deg below T_α are also listed. ^b Value determined at 120°C, the highest temperature at which the HN fit could be conducted in net-PMMA.

determine the individual behavior of the α relaxation in this region as was made in other methacrylate polymers or networks. It has not been possible to build a master curve in this case (Figure 4d). Even in the reduced scales of this plot the shape of the relaxation changes with temperature as characterized by the decrease of the parameter a with temperature; i.e., the distribution of relaxation times becomes narrower with increasing temperature. However, the parameter b seems to be independent of temperature.

The presence of methyl methacrylate units in the copolymer networks shifts the glass transition toward high temperatures with respect to *net*-PBA, the same behavior is shown by DRS, TSDC, and dynamic-mechanical α relaxations. In the dielectric spectrum the increase of the number of MMA units also produces monotonic changes in the strength of the β and α relaxations that makes that COP80 and COP60 show the VFTH behavior in the diagram of Figure 6a, whereas COP40 and COP20 show an Arrhenius behavior. The parameters A , B , and T_0 of the VFTH equation

$$\log f_{\max} = A - \frac{B}{T - T_0} \quad (3)$$

for *net*-PBA, COP80, and COP60 and the apparent activation energies of *net*-PMMA, COP20, and COP40 are shown in Table 1.

TSDC and DMA provide similar results, a single α relaxation is clearly shown in all the copolymers by both techniques, shifting systematically with composition from that of *net*-PBA to that of *net*-PMMA. Figure 8 shows the position of the maximum obtained by both techniques as a function of the copolymer composition. The lines correspond to the Fox equation

$$\frac{1}{T_\alpha} = \frac{w_{BA}}{T_{\alpha BA}} + \frac{w_{MMA}}{T_{\alpha MMA}} \quad (4)$$

w_{PBA} and w_{PMMA} being the weight fractions of BA and MMA in the copolymer, respectively, and T_α the temperature of the maximum corresponding to the main relaxation. The systematic shift of the DMA data to higher temperatures is simply explained by the higher frequency of measurements, 1 Hz against about 10^{-3} Hz in TSDC. It is interesting to note that the α relaxation appears clearly in TSDC in PMMA and the copolymers rich in this component while in DRS the β relaxation is predominant on the α . The same behavior was found in PMMA chain polymer²⁶ and may be due

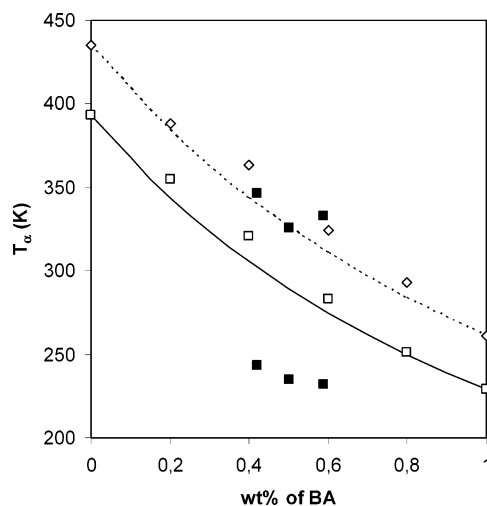


Figure 8. DMA and TSDC peak temperatures T_α for the α relaxation vs weight fraction of PBA in the copolymers, $T_{\alpha DMA}$ (\diamond) and $T_{\alpha TSDC}$ (\square), and the IPNs, $T_{\alpha TSDC}$ (\blacksquare). For the IPNs, both peak temperatures are shown. The lines are best fits of the Fox equation to the copolymer data (full line corresponds to TSDC data and the dotted line to DMA).

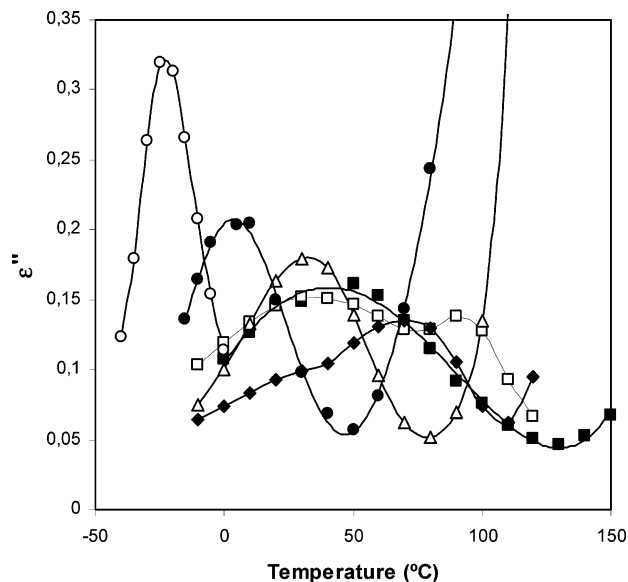


Figure 9. Temperature dependence of the imaginary part of ϵ'' measured at 50 Hz in the polymer and copolymer networks. Symbols are as in Figure 6.

to the contribution of space charge motions in the temperature region of the α relaxation in TSDC and the particular thermal and polarization history by this technique. TSDC measurements with thin insulating foils between the sample and the electrodes to eliminate space charge effects may help in future to further clarify this point.

The influence of the cooperative main relaxation in the DRS relaxation spectrum increases as the fraction of acrylate monomeric units does, as shown by the increase of the relaxation strength. The shape of the isochronous representation of ϵ'' , allows to detect in COP20 and COP40 a double peak whose high-temperature component corresponds to the α relaxation (Figure 9). The analysis of the isothermal curves using the Havriliak–Negami equation did not allow to separate two independent contributions to the overall relaxation process. A single Havriliak–Negami curve could repro-

duce the experimental data in the whole temperature range.

The temperature dependence of the relaxation strength in the copolymers is significantly different from that of the pure *net*-PMMA and *net*-PBA. In the former, the slight increase of $\Delta\epsilon$ is characteristic of a pure β relaxation, region c in the scheme of Figure 1. On the contrary, the rapid increase of $\Delta\epsilon$ with increasing temperature that the copolymers show should correspond to region b in which the α and β relaxations merge. Unfortunately, it has not been possible to characterize the curve $\Delta\epsilon(T)$ at higher temperatures that should correspond to the α region or $\alpha\beta$ relaxation. The shape of the relaxation also reveals some characteristic features in the copolymer networks. The value of the parameter b is independent of temperature in all the copolymers but, except in the case of COP80, the parameter a decreases with temperature the more rapidly the higher is the content of MMA in the copolymer. The values of the HN parameters a and b , corresponding to a temperature 20 degrees below $T_{\alpha\text{DMA}}$, as a function of the copolymer composition have been included in Table 1. It is noteworthy the fact that the value of a varies monotonically with the composition and is greater in the copolymers than in the pure networks showing that the relaxation is broader in the copolymers. This can be due to the fact that the relaxation shown in the copolymers is the superposition of the α and β processes. The presence of compositional heterogeneities along the chain, that may appear as a consequence of a different reactivity of both monomers, could produce the same effect, nevertheless no broadening of the α peak is observed in the loss tangent DMA plot except for the superposition of the β relaxation (Figure 2a).

The shift of the secondary relaxation of PMMA toward lower temperatures with the inclusion of monomeric acrylate units in the chain was already reported in random copolymers of poly(methyl acrylate) and poly(methyl methacrylate) in the 1960s,¹² and it is due to the role played by the methyl groups bonded to the main chain in the hindrance of the rotation of the carboxyl side group that produces the secondary relaxation. This explains the shift of the β relaxation in the series *net*-PMMA–COP20–COP40 as seen in the DRS results. The TSDC results confirm this feature, although only in PMMA and COP20 the position of the β relaxation can be accurately determined (Figure 7).

The IPNs present a broad dynamic-mechanical relaxation region that can be the result of the overlapping of different relaxation processes corresponding to regions rich in *net*-PBA with others rich in *net*-PMMA. Nevertheless, it is clear that there is no relaxation process appearing in the same temperature interval as in the pure networks, which means that due to the high cross-linking density of the networks no region of pure components exists in the IPN with a size larger than the length of cooperativity (a few nanometers^{32–34}). This means that the local composition can be significantly different than the average and consequently there is also a broad dispersion of local glass transition temperatures or local α relaxations along the sample. A similar behavior was shown in similar highly cross-linked sequential IPNs.^{16,17,21,24,25}

The TSDC results also suggest that the IPNs could be phase separated systems with a phase rich in PMMA and a second one rich in PBA. This is indicated on one

hand by the shift of the high-temperature TSDC peak toward the PMMA α peak, with respect to that corresponding to a copolymer with the same composition. On the other hand the shape of the low-temperature peak looks more similar to the PBA α peak rather than the PMMA β peak, in particular for IPN59 (Figure 2) and also in IPN50 (not shown). To further follow this point we included in Figure 8 the peak temperatures of the IPN TSDC peaks that do not fit to the Fox equation.

The dielectric relaxation spectrum in the IPNs shows a single, broad and asymmetric relaxation process with an Arrhenius behavior (Figure 6b). The values of the parameters a and b of the Havriliak–Negami equation are much smaller than those corresponding to the copolymers with the same composition (Table 1). The relaxation shifts toward lower temperatures as the content in *net*-PBA of the IPN increases, analogous to what happens in copolymers COP20 and COP40. Its apparent activation energy is similar to that of *net*-PMMA (Table 1), and the temperature dependence of the relaxation strength also presents the characteristics of a secondary relaxation.

It is worth noting the very different behavior of a copolymer network and an IPN with the same average composition. It seems that in the case of the IPNs the effect of the cooperative α relaxation disappears. This fact can be ascribed to the distribution of the glass transition in a broad temperature interval, what makes that at any temperature only a small part of the chain segments contribute to the cooperative conformational rearrangements that are responsible for the α relaxation. Thus, the characteristics shown by the overall relaxation process are those of the secondary relaxation that predominates in the whole temperature interval.

Conclusions

The crossover scenario in copolymer networks or IPNs containing methyl methacrylate and butyl acrylate monomeric units strongly depends on composition and the nanostructure of the material. Both parameters affect the balance between the strength of the α and β relaxations in the merging region. The *net*-PMMA shows the secondary β relaxation while *net*-PBA shows the cooperative α relaxation. The increase in acrylate units in the copolymer networks increases the strength of the observed relaxation in the copolymers indicating an increase of the participation of the cooperative motions. The copolymer networks present a rapid increase of the relaxation strength with temperature what can be a sign of the merging of α and β relaxations in the crossover region. Nevertheless, a single Havriliak–Negami equation is able to reproduce the experimental ϵ'' isotherms. In the case of the IPNs the relaxation process shown has the characteristics of a secondary relaxation. This feature is ascribed to the fact that the relaxation times of the cooperative motions are distributed in a very broad temperature range.

Acknowledgment. This work was supported by the Spanish Science and Technology Ministry through the MAT2001-2678-C02-01 project (group of the UPV) and by the program “Thales” (NTUA).

References and Notes

- (1) Williams, G. *Trans. Faraday Soc.* **1966**, *62*, 2091.
- (2) Williams, G. *Adv. Polym. Sci.* **1979**, *33*, 60.
- (3) Beiner, M. *Macromol. Rapid Commun.* **2001**, *22*, 869.

- (4) Garwe, F.; Schönhals, A.; Lockwenz, H.; Beiner, M.; Schröter, K.; Donth, E. *Macromolecules* **1996**, *29*, 247.
- (5) Schröter, K.; Unger, R.; Reissig, R.; Garve, F.; Kahle, S.; Beiner, M.; Donth, E. *Macromolecules* **1998**, *31*, 8966.
- (6) Kahle, S.; Korus, J.; Hempel, E.; Unger, R.; Höring, S.; Schröter, K.; Donth, E. *Macromolecules* **1997**, *30*, 7214.
- (7) Beiner, M.; Kahle, S.; Hempel, E.; Schröter, K.; Donth, E. *Macromolecules* **1998**, *31*, 8973.
- (8) Bergman, R.; Alvarez, F.; Alegría, A.; Colmenero, J. *J. Chem. Phys.* **1998**, *109*, 7546.
- (9) Gómez, D.; Alegría, A.; Arbe, K.; Colmenero, J. *Macromolecules* **2001**, *34*, 503.
- (10) Kremer, F.; Schönhals, A. Eds.; *Broadband Dielectric Spectroscopy*; Springer-Verlag: Berlin, 2003.
- (11) Ishida, Y.; Yamafuji, K. *Kolloid Z.* **1961**, *177*, 97.
- (12) McCrum, N. G.; Read, B. E.; Williams, G. *Anelastic and Dielectric Effects in Polymeric Solids*, Dover Publications Inc.: New York, 1991.
- (13) Tetsutani, T.; Kakizaki, M.; Hideshima, T. *Polym. J.* **1982**, *9*, 305.
- (14) Gómez Ribelles, J. L.; Díaz Calleja, R. *J. Polym. Sci., Polym. Phys. Ed.* **1985**, *23*, 1505.
- (15) Gómez Ribelles, J. L.; Meseguer Dueñas, J. M.; Monleón Pradas, M. *J. Appl. Polym. Sci.* **1989**, *38*, 1145.
- (16) Meseguer Dueñas, J. M.; Torres Escuriola, D.; Gallego Ferrer, G.; Monleón Pradas, M.; Gómez Ribelles, J. L.; Pissis, P.; Kyritsis, A. *Macromolecules* **2001**, *34*, 5525.
- (17) Pissis, P.; Kyritsis, A.; Meseguer Dueñas, J. M.; Monleón Pradas, M.; Torres Escuriola, D.; Gallego Ferrer, G.; Gómez Ribelles, J. L. *Macromol. Symp.* **2001**, *171*, 151.
- (18) Vogel, H. *Phys. Z.* **1921**, *22*, 645.
- (19) Fulcher, G. A. *J. Am. Chem. Soc.* **1925**, *8*, 339.
- (20) Tamman, G.; Hesse, W. *Z. Anorg. Allg. Chem.* **1926**, *156*, 245.
- (21) Kyritsis, A.; Gómez Ribelles, J. L.; Meseguer Dueñas, J. M.; Soler Campillo, N.; Gallego Ferrer, G.; Monleón Pradas, M. *Macromolecules* **2004**, *37*, 446.
- (22) Zhang, S.; Jin, X.; Painter, P. C.; Runt, J. *Macromolecules* **2002**, *35*, 3636.
- (23) Cowie, J. M. G.; Ferguson, R.; Fernández, M. D.; Fernández, M. J.; McEwen, I. J. *Macromolecules*, **1992**, *25*, 3170.
- (24) Salmerón M.; Gallego Ferrer, G.; Torregrosa Cabanilles, C.; Meseguer Dueñas, J. M.; Monleón Pradas, M.; Gómez Ribelles, J. L. *Polymer* **2001**, *42*, 10071.
- (25) Gómez Ribelles, J. L.; Meseguer Dueñas, J. M.; Torregrosa Cabanilles, C.; Monleón Pradas, M. *J. Non-Cryst. Solids*, **2002**, *307–310*, 758.
- (26) Van Turnhout, J. In *Topics in Applied Physics: Electrets*; Sessler, G. M., Ed.; Springer: Berlin, 1980; Chapter 3, pp 81–215.
- (27) Havriliak, S.; Negami S. *J. Polym. Sci., Part C: Polym. Symp.* **1966**, *14*, 99.
- (28) Sanchis, M. J.; Díaz Calleja, R.; Gargallo, L.; Hormazabal, A.; Radic, D. *Macromolecules* **1999**, *32*, 3457.
- (29) Leroy, F.; Alegría, A.; Colmenero, J. *Macromolecules* **2002**, *35*, 5587.
- (30) Kyritsis, A.; Pissis, P.; Gomez Ribelles, J. L.; Monleón Pradas, M. *J. Polym. Sci., Part B: Polym. Phys.* **1994**, *32*, 1001.
- (31) Meseguer Dueñas, J. M.; Gomez Ribelles, J. L. Submitted for publication.
- (32) Donth, E. *Relaxation and Thermodynamics in Polymers, Glass Transition*; Akademie Verlag: Berlin, 1992.
- (33) Gómez Ribelles, J. L.; Vidaurre, A.; Cowie, J. M. G.; Ferguson, R.; Harris, S.; McEwen, I. J. *Polymer* **1998**, *40*, 183.
- (34) Gómez Ribelles, J. L.; Monleón Pradas, M.; Meseguer Dueñas, J. M.; Privalko, V. P. *J. Non-Cryst. Solids* **1999**, *244*, 172.

MA049429R